Accelerated Publications

Metal−Phosphate Interactions in the Hammerhead Ribozyme Observed by ^{31}P NMR and Phosphorothioate Substitutions†

Melissa Maderia, Laura M. Hunsicker, and Victoria J. DeRose*

Department of Chemistry, Texas A&M University, College Station, Texas 77842

Received May 31, 2000; Revised Manuscript Received August 10, 2000

ABSTRACT: The hammerhead ribozyme is a catalytic RNA that requires divalent metal cations for activity under moderate ionic strength. Two important sites that are proposed to bind metal ions in the hammerhead ribozyme are the A9/G10.1 site, located at the junction between stem II and the conserved core, and the scissile phosphate (P1.1). ^{31}P NMR spectroscopy in conjunction with phosphorothioate substitutions is used in this study to investigate these putative metal sites. The ^{31}P NMR feature of a phosphorothioate appears in a unique spectral window and can be monitored for changes upon addition of metals. Addition of 1−2 equiv of Cd^{2+} to the hammerhead with an A9-S_{Rp} or A9-S_{Sp} substitution results in a 2−3 ppm upfield shift of the ^{31}P NMR resonance. In contrast, the P1.1-S_{Rp} and P1.1-S_{Sp} ^{31}P NMR features shift slightly and in opposite directions, with a total change in δ of $\leq$0.6 ppm with addition of up to 10 equiv of Cd^{2+}. No significant shifts are observed for an RNA·RNA duplex with a single, internal phosphorothioate modification upon addition of Cd^{2+}. Data obtained using model compounds including diethyl phosphate/thiophosphate, AMP, and AMPS, show that a Cd^{2+}−S interaction yields an upfield shift for the ^{31}P NMR resonance, even in the case of a weak coordination such as with diethyl thiophosphate. Taken together, these data predict that Cd^{2+} has a high affinity for the A9 site and suggest that there is flexibility in metal coordination within the binding pocket. Cd^{2+} interactions with the cleavage site P1.1-S positions are weaker and appear to be stereospecific. These data have implications for mechanisms that have been proposed to explain the influence of metal ions on hammerhead ribozyme activity. These experiments also show the potential utility of ^{31}P NMR spectroscopy in conjunction with phosphorothioates as a probe for metal binding sites in nucleic acids.

Metal ions are critical to both structure and chemical function in RNA[1] molecules (*1*−*4*). Unambiguous identification of important metal ion sites in RNA can be challenging due to multiple binding sites and relatively low affinities, making spectroscopic methods that overcome these problems an important goal. Here we report the use of ^{31}P NMR spectroscopy in conjunction with phosphorothioate substitutions to probe putative metal ion binding sites in the hammerhead ribozyme. Two different sites are investigated that have been predicted to be critical in the reaction catalyzed by this ribozyme. These sites are shown to have very different metal ion affinities, information which can influence mechanistic predictions for hammerhead activity.

Site-specific phosphorothioate labeling of RNA has been used extensively to predict sites of structural and functional importance (*5*−*13*). In particular, phosphorothioate interference experiments are used frequently to probe for metal-binding sites in RNA. Substitution of a specific phosphodiester oxygen by sulfur can dramatically lower the affinity of Mg^{2+} for a putative site, resulting in a decreased activity. In some cases, activity can be rescued by a more thiophilic metal such as Mn^{2+} or Cd^{2+}, and this rescue is generally taken as evidence for a functional metal site in the RNA (*6*, *8*, *9*, *11*, *12*). As has been pointed out (*12*, *14*, *15*), interpretation of these rescue experiments can be complicated by accompanying structural or steric effects caused by the substitution of either the ligand atom or the metal ion.

Here we show that detection by NMR spectroscopy of the well-resolved ^{31}P NMR feature of a phosphorothioate-substituted site provides a convenient method to directly observe putative metal interactions. This technique is demonstrated for two sites in the hammerhead ribozyme, depicted in Figure 1, that have been proposed to bind metal ions on

†This work was supported by the NSF (CAREER), the NIH (GM58096), the Robert A. Welch Foundation, and the Texas Higher Education Coordinating Board Advanced Research Program. V.J.D. is a Cottrell Scholar of the Research Corporation.

* Corresponding author. Phone: 979-862-1401. Fax: 979-845-4719. E-mail: derose@mail.chem.tamu.edu.

[1] Abbreviations: RNA, ribonucleic acid; DNA, deoxyribonucleic acid; NMR, nuclear magnetic resonance; δ, chemical sift; EPR, electron paramagnetic resonance; (site)-S_{Rp} or -S_{Sp}, phosphorothioate substitutions 5′ to the indicated site with R_p or S_p configurations; RNA-OMe, an RNA substrate for the hammerhead riboyzme with a 2′-OCH_3 group on the C17 sugar; TEA, triethanolamine; HEPES, *N*-(2-hydroxyethyl)-piperazine-*N*′-2-ethanesulfonic acid; MES, 2-(*N*-morpholino)ethanesulfonic acid; ENDOR, electron nuclear double resonance; ESEEM, electron spin−echo envelope modulation; TMP, trimethyl phosphate; nt, nucleotide; DEP, diethyl phosphate; DETP, diethyl thiophosphate; AMP, adenosine 5′-monophosphate; AMPS, adenosine 5′-*O*-thiomonophosphate.

10.1021/bi001249w CCC: $19.00
Published on Web 09/13/2000

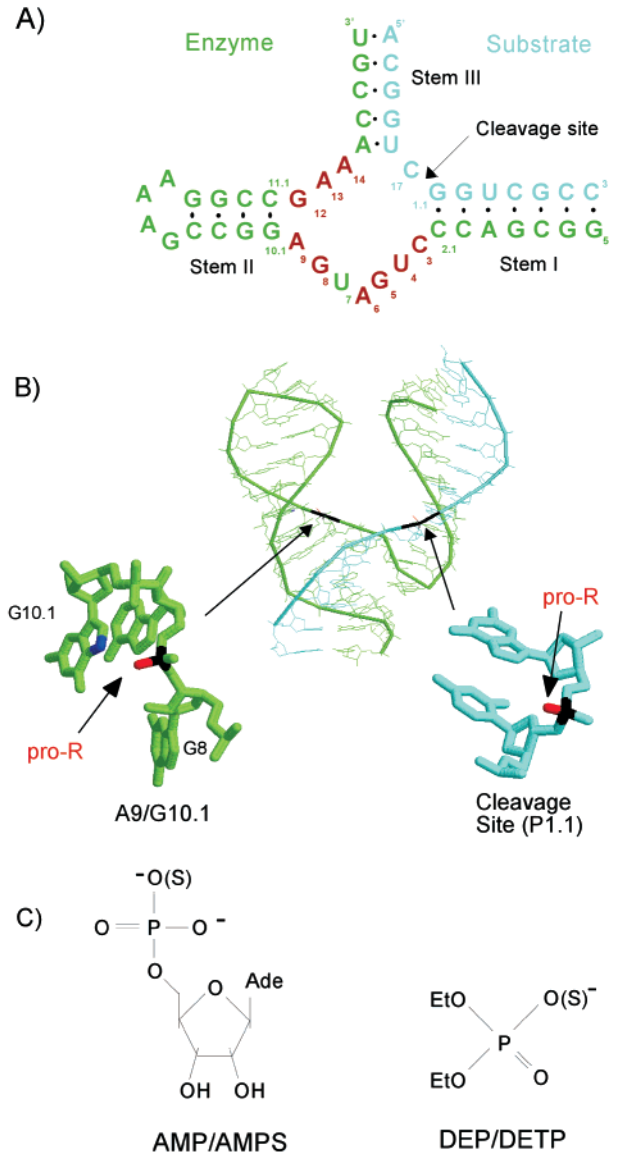

FIGURE 1: Hammerhead ribozyme and model compounds. (A) Hammerhead ribozyme sequence with a 34-nucleotide "enzyme" (green) and a 13-nucleotide "substrate" (cyan) and conserved core nucleotides (red) used in these experiments. Phosphodiester bond cleavage occurs between positions C17 and G1.1 (arrow). (B) X-ray crystal structure of the hammerhead construct (*25*) used in these NMR studies. To the left is the magnified region of the crystal structure for the A9/G10.1 site with the A9 phosphate (black), the *pro-R* oxygen of A9 (red), and the N7 of G10.1 (blue) highlighted. To the right is an enlarged picture of the cleavage site with the *pro-R* oxygen of the scissile phosphate (red) highlighted. Both expanded views are rotated for ease of visualizing the potential M^{2+} ligands. (C) Model compounds, AMP/AMPS (left) and DEP/DETP (right), showing the substitution of one phosphate oxygen atom for a sulfur.

the basis of phosphorothioate substitutions and rescue experiments with thiophilic metal ions. The hammerhead ribozyme reaction is an S_N2-type transesterification wherein the cleavage-site sugar 2′-OH acts as a nucleophile on its 3′ phosphodiester bond, yielding 2′,3′ cyclic phosphate and 5′-OH terminated products (*16*−*18*). Sulfur substitution at the *pro-R* position of the hammerhead scissile bond results in a decrease in Mg^{2+}-dependent activity that can be rescued by more thiophilic metals such as Mn^{2+} (*6*, *8*, *19*−*21*) or Cd^{2+} in a background of Mg^{2+} (*22*, *23*). This result suggests that metal ion coordination at the cleavage site enhances hammerhead activity by decreasing the negative charge at the phosphodiester, although this simple explanation has been questioned (*19*). Phosphorothioate substitution of the *pro-R* oxygen of the A9 phosphate, one proposed ligand in the A9/G10.1 site (Figure 1), also results in a significant decrease of Mg^{2+}-dependent activity which can be rescued in the presence of Cd^{2+} (*8*, *23*, *24*). The role of the A9/G10.1 metal site is intriguing because current crystallographic models (*25*−*27*) show this site to be >15 Å from the cleavage site, and yet activity studies have demonstrated the critical nature of single atoms in this proposed metal-binding pocket (*18*).

Herschlag and co-workers have recently put forth the interesting proposal that the transition state of the hammerhead reaction involves simultaneous metal ion coordination to both the scissile phosphate (denoted as the P1.1 site) and the A9 phosphate (*23*). This proposal is based on measured parameters for Cd^{2+} enhancement of activity when either or both of these sites are substituted with R_p-phosphorothioates. If true, this proposal would require a significant conformational rearrangement from the ground state structures of the hammerhead, the feasibility of which has been disputed by Scott and co-workers (*28*). To shed light on this and other proposed mechanisms for hammerhead ribozyme activity, we have measured the relative effects of Cd^{2+} on both the A9 and the P1.1 site in the hammerhead ribozyme by monitoring their ^{31}P NMR features in phosphorothioate-substituted samples.

MATERIALS AND METHODS

RNA Synthesis and Purification. The unmodified 34-nucleotide (nt) RNA "enzyme" sequence of Figure 1 was synthesized enzymatically using T7 RNA polymerase and purified as described (*29*, *30*). All phosphorothioate substitutions are 5′ from the indicated site and are denoted (site)-$S_{Rp\ or\ Sp}$. Sequences with phosphorothioate substitutions at individual sites were purchased as a mixture of diastereomers [DNA substrate, Integrated DNA Technologies; RNA substrate with 2′-OMe at the cleavage site, 34-nt RNA enzyme with the A9 phosphorothioate, Dharmacon Research (Boulder, CO)]. Diastereomers were separated by HPLC (*20*) with shallower gradients than previously reported to achieve better separation and then dialyzed against the appropriate buffer for 48−72 h. Diastereomer assignments were made by analysis with snake venom phosphodiesterase (*31*). The purity of the isolated diastereomers was assessed by HPLC and ^{31}P NMR spectroscopy to be ≥90% in all cases. For the chemically synthesized 34-nt enzyme strand with an A9-S substitution, less than 40% (see Figure 2A) of the recovered sample had the S_p configuration.

Model Compounds. Diethyl phosphate (DEP) was synthesized from diethyl thiophosphate (DETP, Aldrich) essentially as described (*32*−*34*). DETP (25 μmol) and *m*-chloroperoxybenzoic acid (1 mmol) were reacted in *tert*-butyl alcohol (1 mL total volume) for 36 h at room temperature. Following evaporation of solvent, DEP was resuspended in deionized water and filtered. Purity was analyzed by ^1H and ^{31}P NMR: for ^{31}P, DEP, 1.3 ppm; DETP, 55.3 ppm compared with TMP at 3.7 ppm.

^{31}P NMR Spectroscopy. ^1H-Decoupled ^{31}P NMR spectra of the model compounds were obtained at 121 MHz (300 MHz for ^1H) with a 5 mm quad probe at 24 °C. For RNA samples, ^1H-decoupled ^{31}P NMR spectra were obtained at

Table 1: Effects of Cd^{2+} on ^{31}P NMR Features for Model Compounds and Phosphorothioate-Modified Hammerhead Ribozyme Samples

Model Compounds		
sample	K_d (mM)[a]	Δ (ppm) (direction)[b,c]
AMP	2.5 ± 0.1	2.2 ± 0.3 (+)
AMPS	≤0.4	7.3 ± 0.3 (−)
DEP	NA	NA
DETP	15.2 ± 1.1	1.7 ± 0.1 (−)

Hammerhead Ribozyme Samples		
substrate, Mg^{2+} concn	substitution	Δ (ppm) (direction, equiv of Cd^{2+})[b,d]
RNA-OMe, no Mg^{2+}	A9-R_p	2.2 (−, 1.5)
	A9-S_p	3.2 (−, 1.5)
DNA, 10 mM Mg^{2+}	A9-R_p	2.0 (−, 1)[e]
RNA-OMe, 10 mM Mg^{2+}	P1.1-R_p	0.4 (−, 5)
	P1.1-S_p	0.1 (+, 10)
DNA, no Mg^{2+}	P1.1-R_p	0.6 (−, 10)
	P1.1-S_p	0.3 (+, 10)
DNA, 10 mM Mg^{2+}	P1.1-R_p	0.4 (−, 10)
	P1.1-S_p	0.5 (+, 10)

[a] Apparent K_d's in 0.1 M NaCl, pH 6.0, 25 °C, obtained using eq 1 (see Materials and Methods). [b] Shift directions are indicated as (+) for downfield and (−) for upfield. [c] Values for total chemical shift were obtained using eq 1 and are for saturating Cd^{2+} concentrations. [d] Total chemical shift changes are at the indicated equivalents of Cd^{2+}. Total Cd^{2+} concentration did not exceed 5 mM due to broadening of NMR features and/or pH instability. [e] DNA substrate resulted in incomplete hybrid formation; reported shift is of the feature from the hybrid complex.

202 MHz (500 MHz for ^1H) and 15 °C with an internal coaxial tube containing 5% TMP in D_2O (3.70 ppm) as reference or a Shigemi NMR tube (Shigemi Inc., Allison Park, PA) with an external reference. For model compounds, samples were at 0.4−20 mM in 10 mM MES, pH 6.0. For substitutions at the cleavage site, ^{31}P NMR samples were 200−700 μM total hammerhead concentration in 5 mM HEPES/0.1 M NaCl (pH 8.5) or 5 mM MES/0.1 M NaCl (pH 5.5). ^{31}P NMR spectra of the single-stranded DNA "substrate" in the absence of an enzyme strand show two phosphorothioate resonances for each diastereomer which coalesce to one feature with increasing temperature, indicating that they are due to alternate conformations that are in slow exchange. The diastereomers are ∼>90% pure by C18 chromatography, and in each case a single NMR peak is observed upon addition of an enzyme strand. ^{31}P NMR spectra of single-stranded RNA substrate sequences in the absence of an enzyme strand show a single peak for the ^{31}P NMR feature of the phosphorothioate. For substitutions at the A9 site, NMR samples were 300−500 μM total hammerhead concentration in 5 mM TEA/0.1 M NaCl (pH 7.8). Hammerhead hybrids (denoted as enzyme/substrate) were formed by adding equimolar amounts of enzyme and substrate oligomers, heating to 90 °C for 3 min, and cooling slowly at room temperature. Complete hybrid formation was evident in the NMR experiment by a single phosphorothioate resonance. The A9-S_{Rp}/DNA sample showed two features in the phosphorothioate window, indicating incomplete hybrid formation. Data reported for this sample (Table 1) are only for the ^{31}P NMR feature from the hybrid. In all cases, M^{2+} was added directly to the NMR sample tube from concentrated $CdCl_2$ or $MgCl_2$ stock solutions in water, with no additional annealing step. No changes in pH or sample solubilities were detected during these titrations. ^{31}P NMR spectra for all RNA samples were obtained at 15 °C in order to minimize metal-mediated nonspecific cleavage. Reported rates of cleavage at 15 °C are ∼70% of that at 25 °C (*35*, *36*), indicating that, under the 15 °C NMR experimental conditions, any possible structural changes associated with cleavage should not be inhibited.

*Determination of Equilibrium Dissociation Constant*s. The model compound NMR data were fit (KaleidaGraph, Abelbeck) to eq 1 (*37*) using a simple 1:1 binding model to solve for the equilibrium dissociation constant (K_d) and the total shift for a fully bound C−M^{2+} complex ($[\Delta]_T$).

$$\Delta_{obs} = \frac{[\Delta]_T}{2[C]_T}[(M + [C]_T + K_d) - \sqrt{(M + [C]_T + K_d)^2 - (4M[C]_T)}] \quad (1)$$

In eq 1, $[C]_T$ and M are the total concentration of the model compound and the added metal, respectively, and Δ_{obs} is the observed shift for each data point. Data for hammerhead samples were not fit for an apparent dissociation constant due to complications from the possibility of multiple metal-binding events.

Activity Studies. Hammerhead activity studies were performed as in ref *29* using RNA substrate oligomers labeled with phosphorothioates at the cleavage site (Dharmacon Research, Inc., Boulder, CO; separated and purified as described above). For comparison with NMR studies single-turnover rates were measured at 100 μM hybrid concentration and in the same buffer as used for the NMR samples (5 mM HEPES/0.1 M NaCl, pH 8.5) and 10 mM Mg^{2+}. Measured rates under these conditions: WT, 1.9 min^{-1}; P1.1-S_{Sp}, 0.44 min^{-1}; P1.1-S_{Rp}, <0.001 min^{-1}. Rates measured with addition of 0.25 mM Cd^{2+}: WT, 6.9 min^{-1}; P1.1-S_{Sp}, 0.55 min^{-1}; P1.1-S_{Rp}, 1.66 min^{-1}.

Electrostatic Calculations. The electrostatic calculations were performed essentially as described by Chin et al. (*38*) using a nonlinear Poisson−Boltzmann equation (NLPB). The PDB coordinates of the McKay crystal structure (*25*) include an RNA enzyme strand and a DNA substrate strand. To utilize the NLPB solver (obtained from A. M. Pyle's web site, http://cpmcnet.columbia.edu/dept/gsas/biochem/labs/pyle/electrostatics.html), the two substrate thymine bases were modified by replacing the methyl group of C5 with a proton. Hydrogens were added to the entire structure using the Biopolymers module of Insight II. A phi map was generated using the rna2.crg charge set and the rna2.siz parameter file for atomic radii (Discover Forcefield). The electrostatic surface was visualized using SPOCK (*39*), a program similar to GRASP (*40*), by mapping the calculated charges generated by the NLPB solver onto the surface. Parameters included an internal dielectric constant of 2, an external dielectric constant of 80, and a monovalent concentration of 0.145 M.

RESULTS

Metal Binding at the Hammerhead A9 and Scissile Phosphates. Figure 2A shows the ^{31}P NMR spectra from a mixture of both diastereomers of phosphorothioates at the A9 site of the hammerhead, as well as the isolated R_p isomer. Addition of Cd^{2+} to the mixed isomer sample results in a significant upfield shift for both phosphorothioate features.

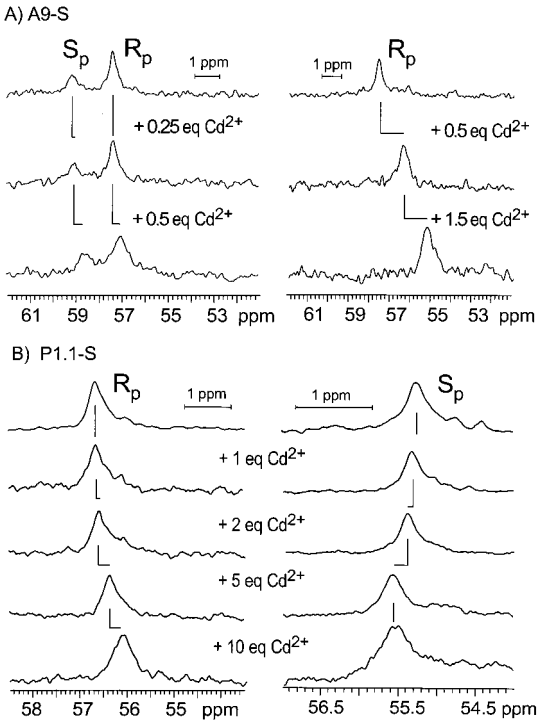

FIGURE 2: ^{31}P NMR spectra of A9-S$_{Rp,Sp}$ or P1.1-S$_{Rp,Sp}$ substitutions in the hammerhead ribozyme. (A) ^{31}P NMR spectra of the A9-S hammerhead with a mixture of both the R_p and S_p isomers (left, 480 μM) in 0, 0.25, and 0.5 equiv of Cd^{2+} and with the isolated R_p isomer (right, 300 μM) in 0, 0.5, and 1.5 equiv of Cd^{2+}. Data are shown for RNA·RNA-OMe hybrids in 5 mM TEA, pH 7.8, and 100 mM NaCl at 15 °C. (B) ^{31}P NMR spectra of the RNA·DNA hybrids having a single phosphorothioate substitution at the cleavage site [P1.1-S$_{Sp}$ isomer at right (550 μM), P1.1-S$_{Rp}$ isomer at left (332 μM)]. Data are shown with addition of 0, 1, 2, 5, and 10 equiv of Cd^{2+} in 5 mM HEPES, pH 8.5, and 100 mM NaCl at 15 °C.

Similar results were observed with both the isolated A9-S$_{Rp}$ (2A, right) and A9-S$_{Sp}$ (data not shown) hammerheads, resulting in shifts of 2−3 ppm with only 1−1.5 equiv of added Cd^{2+}, indicating that Cd^{2+} binds with relatively high affinity to this site. The upfield shift direction in the ^{31}P NMR features with Cd^{2+} addition is consistent with previously observed Cd−phosphorothioate interactions (*41*−*44*; see below). This shift direction is the opposite of that observed with most metal−phosphate binding events, which may be due to the more covalent nature of the Cd^{2+}−sulfur bond.

When the same experiment is performed for phosphorothioate substitutions at the cleavage site of the hammerhead, a dramatically different result is observed (Figure 2B). The results of Cd^{2+} addition to the hammerhead with separated P1.1-S R_p and S_p diastereomers are shown in Figure 2B. A small shift of ≤0.6 ppm is observed in these ^{31}P NMR features over the range of 1−10 equiv of added Cd^{2+}. Moreover, the shifts are in opposite directions for the two diastereomers. The signal from the R_p diastereomer shifts upfield, as expected for a Cd^{2+} interaction with sulfur in the phosphorothioate. By contrast, a small shift *downfield* is observed when Cd^{2+} is added to the S_p diastereomer. This downfield shift could indicate that Cd^{2+} coordinates, unexpectedly, to oxygen in the S_p-phosphorothioate. Alternatively, the NMR shift in the S_p sample may be due to a conformational change rather than, or in addition to, direct binding of Cd^{2+} to the sulfur of the thiophosphate.

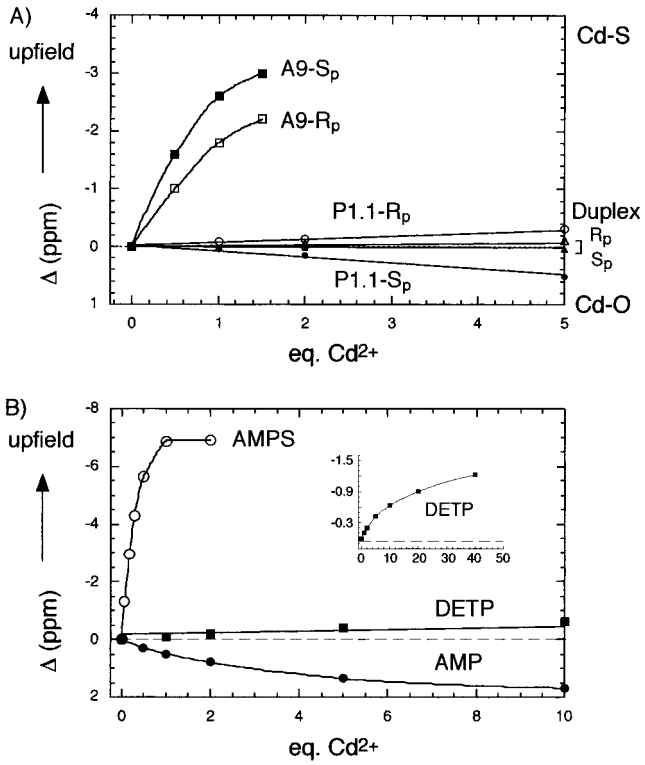

FIGURE 3: Cd^{2+}-induced ^{31}P chemical shift changes in the hammerhead ribozyme and model compounds. (A) The total change in the ^{31}P chemical shift [Δ (ppm)] and the direction of the shift are plotted as a function of added Cd^{2+} for the phosphorothioate-substituted site in both the A9-S$_{Rp}$ (□) and A9-S$_{Sp}$ (■) hammerhead samples (isolated isomers; see Materials and Methods), P1.1-S$_{Rp}$ (○) and P1.1-S$_{Sp}$ (●) samples (data of Figure 2), and RNA·RNA 13-nt duplex samples containing a single internal R_p- (△) or S_p- (▲) phosphorothioate modification. (B) Δ (ppm) for the ^{31}P shift in the model compounds DETP (■), AMPS (○), and AMP (●) with added Cd^{2+} (conditions described in Materials and Methods).

The very different effects of metal ions on the A9 site and on the cleavage site are displayed graphically in Figure 3A. These results can be compared with results (Figure 3B) from similar experiments using the phosphate and phosphorothioate-containing model compounds such as those shown in Figure 1C. Two important control experiments enhance interpretation of the results obtained for the ribozyme. It is important to demonstrate that phosphorothioate−Cd^{2+} interactions in oligonucleotides are not induced simply by placement of the sulfur at random positions in the RNA. The ^{31}P NMR spectrum of a phosphorothioate embedded in the middle of a 13-nt RNA duplex showed only minimal effects upon addition of Cd^{2+} (Figure 3A). Similar results were obtained for single phosphorothioates in single-stranded RNA and DNA oligomers, as well as 5′ to G1.5 in stem I of the hammerhead ribozyme (data not shown). Thus, phosphorothioate substitution alone is insufficient to create a high-affinity Cd^{2+} site in these RNAs.

The upfield ^{31}P chemical shift change accompanying Cd−phosphorothioate complexation is observed for ATPαS (*42*, *43*), as well as in a phosphorothioate-substituted GAAA tetraloop (*44*). It is important to confirm that this effect can be ascribed to a Cd^{2+}−sulfur interaction and is not in reality caused by some conformational change induced by simultaneous coordination to a nucleic acid base. To this end, Cd^{2+} binding to the simple model compound diethyl thiophosphate

was investigated in comparison with diethyl phosphate. ^{31}P NMR spectra of diethyl thiophosphate show an upfield shift as expected upon binding of Cd^{2+} to the sulfur (Figure 3B), with an apparent K_d for Cd^{2+} of 15 mM for this interaction in 0.1 M NaCl, pH 6.0, 25 °C (Table 1). The same experiment with diethyl phosphate, lacking the sulfur ligand, showed *no* apparent Cd^{2+}−phosphate interactions over the concentration range available in the NMR experiment (up to 50 mM Cd^{2+}). Comparison of Cd^{2+} binding to AMPS and AMP also shows the expected upfield and downfield ^{31}P shifts from Cd−S and Cd−O coordination, respectively (Table 1). Affinities of Cd^{2+} for AMP and AMPS measured in this way [Table 1: K_d(AMP) = 2.5 ± 0.1 mM; K_d(AMPS) ≤ 0.4 mM (pH 6.0, 0.1 M NaCl)] are in reasonable agreement with those reported by Sigel and co-workers [K_d(AMP) = 1.8 mM; K_d(AMPS) = 0.023 mM (I = 0.1 M, $NaNO_3$)] (*45*). Sigel and co-workers also calculate >90% coordination of Cd^{2+} to sulfur in AMPS (*45*), consistent with the upfield shift in the ^{31}P NMR feature (Figure 3, Table 1). The higher affinities of Cd^{2+} for AMP and AMPS over those for the simple phosphodiester/phosphorothioate compounds reflect the influence of Cd^{2+}−base interactions (*45*) and/or the effect of an additional negative charge in the nucleotide models.

The hammerhead experiments in Figure 2 were performed in the presence of 0.1 M NaCl, which is expected to support duplex formation and possibly additional folding in the ribozyme samples. Similar results were observed when 10 mM Mg^{2+} was added to either the A9 or P1.1 phosphorothioate-substituted hammerhead samples prior to titration with Cd^{2+}, indicating that any additional core folding induced by divalent cations (in 0.1 M NaCl) does not influence these results (Table 1). The effect of substituents at the 2′-position of C17, required to inhibit cleavage activity during the NMR experiments, was also investigated. Essentially the same results were observed if the phosphorothioate-containing substrate strand was an all-DNA strand or an all-RNA substrate with a 2′-OMe substitution at the cleavage site. These results are summarized in Table 1.

DISCUSSION

The results described here provide information concerning metal interactions at two different sites of the hammerhead ribozyme. Cd^{2+} has been demonstrated to rescue the inhibitory effect of an R_p-phosphorothioate substitution at the A9 site (*23*, *24*) and at the hammerhead cleavage site (*22*, *23*). The ^{31}P NMR data presented here indicate that the affinity of Cd^{2+} for the A9 site is relatively high, reaching saturation with addition of ~2 equiv of Cd^{2+} to these NMR samples (K_d ≤ 300 μM). By contrast, the Cd^{2+} interaction with phosphorothioates at the cleavage site appears to be considerably weaker, exhibiting properties more similar to those observed for simple diethyl thiophosphate. As discussed below, these data have implications for mechanisms that have been proposed to explain the influence of metal ions on hammerhead ribozyme activity.

Properties of Metal Binding to the A9 and P1.1 Sites. The stereospecificity of Cd^{2+} for ligands at these two hammerhead sites is of interest. Addition of Cd^{2+} causes large ^{31}P NMR shifts in the upfield direction for both the A9-S_{Rp} and A9-S_{Sp} samples (Figure 2A). These data suggest that, in the ground state structure of the hammerhead, Cd^{2+} binds sulfur whether it is substituted in the *pro-R* position or the *pro-S* position of the phosphodiester at A9. This result is somewhat surprising since previous work has provided evidence only that the *pro-R* position provides a ligand to metal ions involved in hammerhead activity. Neither Mg^{2+} (*23*, *24*) nor Mn^{2+} (DeRose and Hunsicker, unpublished) support full activity in the A9-S_{Rp} hammerhead, whereas Cd^{2+} can fully rescue activity for this substitution; these data provide strong evidence for functional significance of metal coordination to the *pro-R* position of the A9 site. In the A9-S_{Sp} hammerhead, Cd^{2+}, Mg^{2+}, and Mn^{2+} all support activity. It is most likely that the relatively hard Mg^{2+} and Mn^{2+} coordinate to oxygen in the A9-S_{Sp} sample. It is possible, however, that the larger ionic radius and increased thiophilicity of Cd^{2+} allow this ion to bind to sulfur in the A9-S_{Sp} sample, as is suggested by the NMR data of Figure 2A. Further experiments will be required to confirm that this binding mode has functional significance.[2]

At the hammerhead cleavage site (P1.1), it is interesting that Cd^{2+} addition to the R_p- and S_p-phosphorothioate diastereomers results in ^{31}P chemical shift changes in opposite directions. It is possible that these different shift directions reflect the fact that thiophilic Cd^{2+} binds to the *pro-R* position in both samples, whether it is oxygen or sulfur. Such a result would suggest that the thiophilicity of Cd^{2+} is overcome through the influence of additional metal−RNA interactions around the P1.1 *pro-R* position. In X-ray crystal structures of both RNA·DNA (*25*) and RNA·RNA hammerhead models (*26*, *27*), the cleavage site phosphodiester bond lies at the edge of a cavity created by stems I and II (Figure 4). The *pro-R* oxygen of the scissile phosphodiester is positioned toward the inside of the stem I/stem II cavity with no obvious additional metal ligands, whereas the *pro-S* oxygen faces away from this cavity. While no metal ion is found bound to the scissile phosphate in "ground state" crystal structures, Scott and co-workers have reported a metal interaction with the *pro-R* position of the cleavage site in a structure that was trapped upon elevating the pH in crystals of a "slow-cleaving" hammerhead (*46*). Consistent with their report, the Cd^{2+}-induced shifts of the cleavage-site phosphorothioate ^{31}P NMR spectra were observed at pH 8.5 (Figure 2B) but not at pH 5.5 (data not shown).

An electrostatic surface plot of the hammerhead (Figure 4) shows that the interior of the cavity formed by stems I and II has regions of relatively high negative charge, with a particularly high density around the A9/G10.1 site. The multiple regions of negative charge density may serve to "trap" positive ions and also be a contributing factor in directing cations to the *pro-R* position of the hammerhead scissile phosphate. Such a trap for divalent cations has recently been proposed on the basis of the results of Brownian dynamics simulations of metal−RNA interactions in the hammerhead (*47*). The high apparent affinity of metals for the A9/G10.1 site is likely contributed to by local

[2] It should be noted that while shifts in the P9-S ^{31}P NMR features observed with Cd^{2+} addition are in the direction and of the magnitude expected for metal ion coordination, this conclusion is not unequivocal. It remains possible that shifts in the ^{31}P NMR features are caused by a large conformational change induced by metal coordination to a different site. While we regard this as a less likely scenario because of the magnitude (>2 ppm) of the ^{31}P shifts, independent confirmation of metal coordination using other techniques is also being pursued.

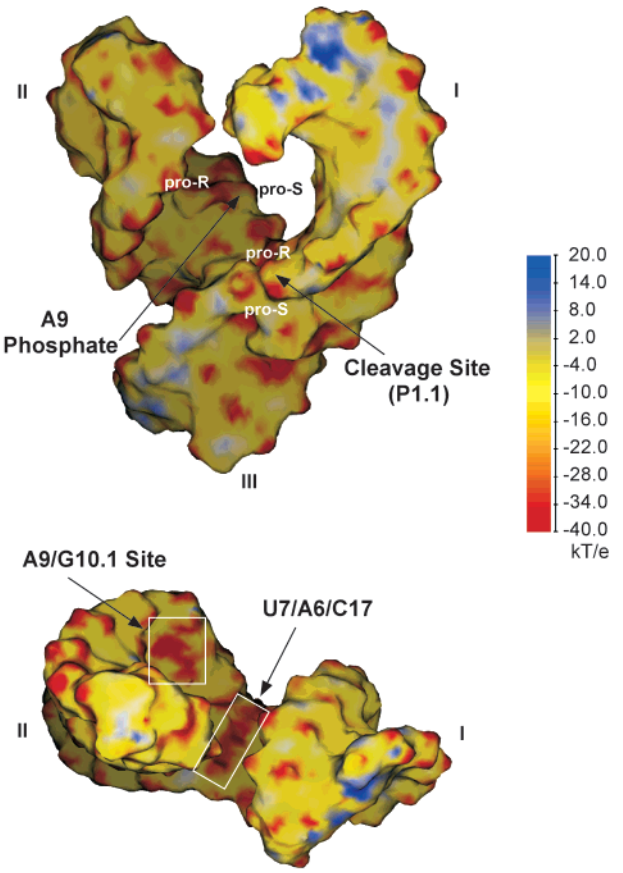

FIGURE 4: Electrostatic surface image of the RNA·DNA hammerhead ribozyme. The electrostatic surface was generated using coordinates (Brookhaven Protein Data Bank entry 1HMH) for the RNA·DNA hammerhead (*25*) of Figure 1 and the NLPB Solver (*38*) and visualized using SPOCK (*39*). Colors indicate relative charges of 20 kT/e (blue) to −10 kT/e (yellow) to −40 kT/e (red). Upper figure, front view: Arrows indicate the cleavage site and the A9/G10.1 site, and the *pro-R* and *pro-S* positions of these sites have been denoted. Lower figure, top view looking down stems I and II: Boxes denote regions of negative surface charge for the A9/G10.1 site and also the cleft between stems I and II with contributions from U7/A6/C17.

electrostatics and possibly a preformed binding pocket that places the A9 phosphate and N7 of G10.1 in close proximity.

Implications for the Mechanism of Hammerhead Cleavage. The results described here support a picture in which the A9/G10.1 site is populated at low concentrations of metal ions, whereas the scissile phosphate has a relatively weak interaction with metal ions. Below, these results are considered in light of two scenarios describing the influence of metals on hammerhead activity.

Much of the available data from activity and other measurements on the hammerhead ribozyme can be fit to a model in which activity is influenced by separate effects of metals at the A9/G10.1 site, the scissile phosphate, and at least one other position. Most studies in which hammerhead activity is monitored as a function of added Mg^{2+} or Mn^{2+} show that maximum activity requires relatively high concentrations of metal ions (*3*, *4*, *6*, *29*, *48*). On the basis of the concentration of metal ion that is required to reach half-maximum activity, these experiments indicate that there is at least one critical metal ion that has an apparent $K_d \sim 1-10$ mM. We have directly measured Mn^{2+} binding to the hammerhead ribozyme in solution conditions using EPR spectroscopy (*29*) and find high-affinity ($K_d \leq 10$ μM, 0.1−1.0 M NaCl) as well as low-affinity Mn^{2+} sites. For one of these high-affinity sites, ENDOR (*49*) and ESEEM (*50*) spectroscopies have allowed identification of ligands that are consistent with the A9/G10.1 site. This site is populated at low Mn^{2+} concentrations with an apparent affinity of $K_d \leq 10$ μM in both 0.1 and 1.0 M NaCl. Hammerhead activity still requires >1 mM Mn^{2+}, however, meaning that population of a different, relatively low-affinity metal site(s) also is required. Since Hill coefficients of >1 are measured for Mg^{2+} and Mn^{2+}-associated hammerhead activity (6), there may be more than one type of metal ion interaction with this apparent low affinity.

On the basis of the results of the NMR study presented here, the cleavage site *pro-R* oxygen is one possible candidate for the second, weak-affinity metal ion site that is critical for hammerhead activity. Another candidate for a functional low-affinity site is found in results reported by Lilley and co-workers, who observe a hammerhead folding event that requires 1−10 mM Mg^{2+} (*51*−*53*). Even in 1 M NaCl, however, where hammerhead folding requirements from general charge shielding should be satisfied, Mn^{2+}-supported activity still requires metal ion concentrations of >4 mM Mn^{2+} (*29*). In addition, we recently reported evidence that $Co(NH_3)_6^{3+}$ inhibits hammerhead activity by binding at a site that does not appear to be the A9/G10.1 site (*54*) and that this inhibition is reversible with added Mn^{2+}. Taken together, these observations suggest that while the A9/G10.1 site is critical to hammerhead activity, population of at least one additional divalent metal site also is required.

In a novel hypothesis based on recent experimental results, Herschlag and co-workers have proposed what can be termed a "rearrangement" mechanism for hammerhead activity (*23*). In this mechanism, the metal ion bound at the A9/G10.1 site is predicted to also interact with the *pro-R* oxygen at the cleavage site, requiring a large conformational change that precedes the transition state of the reaction. This proposal is based on apparent K_d's that have been measured for Cd^{2+} rescue of activity in phosphorothioate-substituted samples in a background of Mg^{2+}. From the Cd^{2+} enhancement of activity, similar apparent K_d's of >200 μM (10 mM $MgCl_2$, pH 6.5) were derived for both the WT hammerhead and the P1.1-S_{Rp}-substituted sample. A lower Cd^{2+} K_d of <80 μM is reported for the A9-S_{Rp} hammerhead, and the same apparent K_d was measured for the double-substituted A9-S_{Rp}/P1.1-S_{Rp} hammerhead. From these experiments, it is concluded that in each case the apparent affinity measured by the rise in activity reflects Cd^{2+} binding only to the A9/G10.1 site in the ground state of the ribozyme. Because the expected increased affinity of Cd for the P1.1-S_{Rp} site is not reflected in these measurements, that interaction is predicted to occur only in the transition state of the reaction. Similar experimental results with a slightly different interpretation have also been reported by Yoshinari and Taira (*55*).

One experimental prediction drawn from the rearrangement model is that, for the ground state hammerhead structure, metal ions might bind with a high affinity to the A9 site but have no interaction with the cleavage site (*23*). These predictions are generally met by the observations in this ^{31}P NMR study in that a relatively large shift that saturates with added Cd^{2+} is observed at the A9 site, and the interaction with the cleavage site is apparently weak. It

is not obvious, however, that the samples used in these NMR experiments would remain predominantly in the ground state configuration. Thus it might be surprising that no large shifts are observed in the P1.1-S_{Rp} sample since, given that from the predicted (*23*) K_d's, the unmodified A9/G10.1 site is expected to be populated with addition of a few equivalents of Cd^{2+} to the (>400 μM RNA) NMR samples.

The following are possible scenarios by which the "rearrangement" hypothesis might be consistent with the present NMR data: (a) Population of the "closed" conformation induces only minor changes in the phosphodiester backbone geometry of the scissile phosphate, resulting in the small change in the chemical shift of the P1.1 feature. (b) The large conformational change is somehow blocked by the 2′-OH modifications used in the substrate strand in these NMR experiments. (c) The hammerhead ribozyme is in a fast exchange between the closed conformational state, in which the A9 and P1.1 phosphates are in close proximity, and the "open" or ground state structure. In scenario (c), if the closed structure is significantly less populated, then the result would be the smaller change in the ^{31}P NMR signal of the P1.1-S as is observed (<0.6 ppm). Also, in this transiently populated closed conformation, if the metal coordinating at the A9/G10.1 site adopts the *pro-R* oxygen of the scissile phosphate as an additional ligand, then this would result in stereoselectivity at the cleavage site phosphate. These three scenarios, (b) or (c) seeming the most plausible, are ways to reconcile the present experimental observations with the model proposed by Wang et al.

General Utility of P-S ^{31}P NMR for Investigating Metal Binding in RNA. Several methods are currently used to measure apparent metal ion affinities in structured RNAs under solution conditions. CD (*56*−*59*) and fluorescence spectroscopies (*51*−*53*, *60*, *61*), thermodynamic measurements (*1*, *14*, *54*, *62*−*64*), free radical footprinting (*65*−*68*), and small-angle scattering (*69*) experiments are important tools in analyzing the effects of metal ions on global RNA conformation. With these techniques, however, it is difficult to identify a specific metal ligand in the RNA. Pardi and coworkers recently demonstrated the use of ^{31}P NMR to measure Mg^{2+} affinity for a site involving the A13 P of the hammerhead ribozyme (*70*). These experiments were possible because the ^{31}P NMR feature from this site is resolved from the otherwise unresolved ^{31}P envelope and could be identified using ^{17}O substitution. ^1H NOE's from $Co(NH_3)_6^{3+}$ (*37*, *71*−*74*) and paramagnetic broadening from Mn^{2+} (*70*, *75*−*77*) are both important methods to locate metal sites and have been used in a number of RNAs. Luminescence experiments for detecting Tb^{3+} and Eu^{3+} binding sites have also been described (*78*). An interesting new prospect for monovalent ions is the ^{205}Tl NMR technique recently described by Strobel and co-workers (*79*). We have used Mn^{2+} EPR (*29*) and related techniques, including ENDOR (*49*) and ESEEM (*50*), to identify metal ion ligands, which is possible when Mn^{2+} can be placed in one or a limited number of sites.

Among these techniques, ^{31}P NMR of phosphorothioate substitutions is useful in that the substituted RNA site is immediately observable, with a signal that is sensitive to metal ion binding. The influence of thiophilic Cd^{2+} can be observed in a background of other ions, which may be important to support folding in the RNA under investigation. It is important to note, however, that some phosphorothioate substitutions can also cause structural changes (*14*, *15*, *44*) and that independent methods may be required to characterize the substituted RNA. In the two substitutions described here, such effects appear minimal since Cd^{2+} addition supports full activity. This technique is therefore a useful method to establish relative metal ion affinities at different sites in the hammerhead ribozyme.

ACKNOWLEDGMENT

We thank Dr. Susan Morrissey and Steve Silber for assistance in NMR data acquisition and the reviewers for helpful suggestions.

NOTE ADDED IN PROOF

Suzumura et al. (*80*) reported recently that attempts to observe phosphorothioate ^{31}P NMR signals from the hammerhead P9 position were unsuccessful at temperatures <60 °C due to proposed conformational fluctuations. The hammerhead sequence used in this study has a longer stem I (Figure 1), which may explain our ability to observe such signals.

REFERENCES

1. Misra, V. K., and Draper, D. E. (1999) *Biopolymers 48*, 113−135.
2. Pyle, A. M. (1993) *Science 261*, 709−714.
3. Cech, T. R. (1993) in *The RNA World* (Gesteland, R., and Atkins, J., Eds.) pp 239−270, Cold Spring Harbor Laboratory Press, Cold Spring Harbor, NY.
4. Pan, T., Long, D. M., and Uhlenbeck, O. C. (1993) in *The RNA World* (Gesteland, R., and Atkins, J., Eds.) pp 271−302, Cold Spring Harbor Laboratory Press, Cold Spring Harbor, NY.
5. Narlikar, G. J., and Herschlag, D. (1997) *Annu. Rev. Biochem. 66*, 19−59.
6. Dahm, S. C., and Uhlenbeck, O. C. (1991) *Biochemistry 30*, 9464−9469.
7. Ruffner, D. E., and Uhlenbeck, O. C. (1990) *Nucleic Acids Res. 18*, 6025-6029.
8. Knoll, R., Bald, R., and Furste, J. P. (1997) *RNA 3*, 132−140.
9. Sood, V. D., Beattie, T. L., and Colins, R. A. (1998) *J. Mol. Biol. 282*, 741−750.
10. Christian, E. L., and Yarus, M. (1992) *J. Mol. Biol. 228*, 743−758.
11. Christian, E. L., and Yarus, M. (1993) *Biochemistry 32*, 4475−4480.
12. Basu, S., and Strobel, S. A. (1999) *RNA 5*, 1399−1407.
13. Boudvillain, M., and Pyle, A. M. (1998) *EMBO J. 17*, 7091−7104.
14. Horton, T. E., Maderia, M., and DeRose, V. J. (2000) *Biochemistry 39*, 8201−8207.
15. Smith, J. S., and Nikoniwicz, E. P. (2000) *Biochemistry 39*, 5642−5652.
16. Bratty, J., Chartrand, P., Ferbeyre, G., and Cedergren, R. (1993) *Biochim. Biophys. Acta 1216*, 345−359.
17. Wedekind, J. E., and McKay, D. B. (1998) *Annu. Rev. Biophys. Biomol. Struct. 27*, 475−502.
18. McKay, D. B. (1996) *RNA 2*, 395−403.
19. Zhou, D. M., He, Q. C., Zhou, J. M., and Taira, K. (1998) *FEBS Lett. 431*, 154−160.
20. Slim, G., and Gait, M. J. (1991) *Nucleic Acids Res. 19*, 1183−1188.
21. Buzayan, J. M., van Tol, H., Feldstein, P. A., and Bruening, G. (1990) *Nucleic Acids Res. 18*, 4447−4451.
22. Scott, E. C., and Uhlenbeck, O. C. (1999) *Nucleic Acids Res. 27*, 479−484.
23. Wang, S., Karbstein, K., Peracchi, A., Beigelman, L., and Herschlag, D. (1999) *Biochemistry 38*, 14363−14378.

24. Peracchi, A., Beigelman, L., Scott, E. C., and Uhlenbeck, O. C. (1997) *J. Biol. Chem. 272*, 26822−26826.
25. Pley, H. W., Flaherty, K. M., and McKay, D. B. (1994) *Nature 372*, 68−74.
26. Scott, W. G., Finch, J. T., and Klug, A. (1995) *Cell 81*, 991−1002.
27. Murray, J. B., Terwey, D. P., Maloney, L., Karpeisky, A., Usman, N., Beigelman, L., and Scott, W. G. (1998) *Cell 92*, 665−673.
28. Murray, J. B., and Scott, W. G. (2000) *J. Mol. Biol. 296*, 33−41.
29. Horton, T. E., Clardy, D. R., and DeRose, V. J. (1998) *Biochemistry* 18094−18101.
30. Milligan, J. F., and Uhlenbeck, O. C. (1989) *Methods Enzymol. 180*, 51−62.
31. Griffiths, A. D., Potter, B. V. L., and Eperon, I. C. (1987) *Nucleic Acids Res. 15*, 4145−4162.
32. Wu, S.-Y., Segall, Y., Sanders, M., Toia, R. F., and Casida, J. E. (1990) *Phosphorus Sulfur 54*, 221−224.
33. Segall, Y., and Casida, J. E. (1983) *Phosphorus Sulfur 18*, 209−212.
34. Segall, Y., Wu, S.-Y., Toia, R. F., and Casida, J. E. (1990) *Tetrahedron Lett. 31*, 473−476.
35. Peracchi, A. (1999) *Nucleic Acids Res. 27*, 2875−2882.
36. Hertel, K. J., and Uhlenbeck, O. C. (1995) *Biochemistry 34*, 1744−1749.
37. Gonzalez, R. L., and Tinoco, I. (1999) *J. Mol. Biol. 289*, 1267−1282.
38. Chin, K., Sharp, K. A., Honig, B., and Pyle, A. M. (1999) *Nat. Struct. Biol. 6*, 1055−1061.
39. Christopher, J. (1998) *SPOCK: The Structural Properties Observation and Calculation Kit (Program Manual)*, Center for Macromolecular Design, Texas A&M University, College Station, TX.
40. Nicholls, A., Sharp, K. A., and Honig, B. (1991) *Proteins 11*, 281−296.
41. Eckstein, F. (1985) *Annu. Rev. Biochem. 54*, 367−402.
42. Jaffe, E. K., and Cohn, M. (1978) *Biochemistry 17*, 652−657.
43. Pecoraro, V. L., Hermes, J. D., and Cleland, W. W. (1984) *Biochemistry 23*, 5262−5271.
44. Maderia, M., Horton, T. E., and DeRose, V. J. (2000) *Biochemistry 39*, 8193−8200.
45. Sigel, H. (1997) *J. Am. Chem. Soc. 119*, 744−755.
46. Scott, W. G., Murray, J. B., Arnold, J. R. P., Stoddard, B. L., and Klug, A. (1996) *Science 274*, 2065−2069.
47. Hermann, T., and Westhof, E. (1998) *Structure 6*, 1303−1314.
48. Hunsicker, L. M., and DeRose, V. J. (2000) *J. Inorg. Biochem.* (in press).
49. Morrissey, S. R., Horton, T. E., and DeRose, V. J. (2000) *J. Am. Chem. Soc. 122*, 3473−3481.
50. Morrissey, S. R., Horton, T. E., Grant, C. V., Hoogstraten, C. G., Britt, R. D., and DeRose, V. J. (1999) *J. Am. Chem. Soc. 121*, 9215−9218.
51. Bassi, G. S., Murchie, A. I. H., and Lilley, D. M. J. (1996) *RNA 2*, 756−768.
52. Bassi, G. S., Murchie, A. I. H., Walter, F., Clegg, R. M., and Lilley, D. M. J. (1997) *EMBO J. 16*, 7481−7489.
53. Bassi, G. S., Møllegaard, N. E., Murchie, A. I. H., and Lilley, D. M. J. (1999) *Biochemistry 38*, 3345−3354.
54. Horton, T. E., and DeRose, V. J. (2000) *Biochemistry 39*, 11408−11416.
55. Yoshinari, K., and Taira, K. (2000) *Nucleic Acids Res. 28*, 1730−1742.
56. Fang, X., Pan, T., and Sosnick, T. R. (1999) *Biochemistry 38*, 16840−16846.
57. Pan, T., and Sosnick, T. R. (1997) *Nat. Struct. Biol. 4*, 931−938.
58. Hashem, G. M., Pham, L., Vaughan, M. R., and Gray, D. M. (1998) *Biochemistry 37*, 61−72.
59. Clark, C. L., Cecil, P. K., Singh, D., and Gray, D. M. (1997) *Nucleic Acids Res. 25*, 4098−4105.
60. Qin, P. Z., and Pyle, A. M. (1997) *Biochemistry 36*, 4718−4730.
61. Singh, K. K., Parwaresch, R., and Krupp, G. (1999) *RNA 5*, 1348−1356.
62. Gluick, T. C., Wills, N. M., Gesteland, R. F., and Draper, D. E. (1997) *Biochemistry 36*, 16173−16186.
63. Nixon, P. L., and Giedroc, D. P. (1998) *Biochemistry 37*, 16116−16129.
64. Nixon, P. L., Theimer, C. A., and Giedroc, D. P. (1999) *Biopolymers 50*, 443−458.
65. Rosenstein, S. P., and Been, M. D. (1996) *Biochemistry 35*, 11403−11413.
66. Chaulk, S. G., and MacMillan, A. M. (2000) *Biochemistry 39*, 2−8.
67. Hampel, K. J., Walter, N. G., and Burke, J. M. (1998) *Biochemistry 37*, 14672−14682.
68. Sclavi, B., Woodson, S., Sullivan, M., Chance, M. R., and Brenowitz, M. (1997) *J. Mol. Biol. 266*, 144−159.
69. Russell, R., Millett, I. S., Doniach, S., and Herschlag, D. (2000) *Nat. Struct. Biol. 7*, 367−370.
70. Hansen, M. R., Simorre, J. P., Hanson, P., Mokler, V., Bellon, L., Beigelman, L., and Pardi, A. (1999) *RNA 5*, 1099−1104.
71. Gdaniec, Z., Sierzputowska-Gracz, H., and Theil, E. C. (1998) *Biochemistry 37*, 1505−1512.
72. Butcher, S. E., Allain, F. H. T., and Feigon, J. (2000) *Biochemistry 39*, 2174−2182.
73. Rüdisser, S., and Tinoco, I. (2000) *J. Mol. Biol. 295*, 1211−1223.
74. Kieft, J. S., and Tinoco, I. (1997) *Structure 5*, 713−721.
75. Moldrheim, E., Andersen, B., Frøystein, N. Å., and Sletten, E. (1998) *Inorg. Chim. Acta 273*, 41−46.
76. Hud, N. V., and Feigon, J. (1997) *J. Am. Chem. Soc. 119*, 5756−5757.
77. Hurd, R. E., Azhderian, E., and Reid, B. R. (1979) *Biochemistry 18*, 4012−4017.
78. Feig, A. L., Panek, M., Horrocks, W. DeW., and Uhlenbeck, O. C. (1999) *Chem. Biol. 6*, 801−810.
79. Basu, S., Szewczak, A. A., Cocco, M., and Strobel, S. A. (2000) *J. Am. Chem. Soc. 122*, 3240−3241.
80. Suzumura, K., Warashina, M., Yoshinara, K., Tanaka, Y., Kuwabara, T., Orita, M., and Taira, K. (2000) *FEBS Lett. 473*, 106−112.

BI001249W